Cell-selective intracellular delivery of a foreign enzyme to endothelium *in vivo* using vascular immunotargeting

ARNAUD SCHERPEREEL,*[,1] RAINER WIEWRODT,*[1]
MELPO CHRISTOFIDOU-SOLOMIDOU,* RADJ GERVAIS,* JUAN-CARLOS MURCIANO,[†]
STEVEN M. ALBELDA,* AND VLADIMIR R. MUZYKANTOV[†,‡,2]

*Pulmonary, Allergy and Critical Care Division, Department of Medicine, [†]Institute of Environmental Medicine and [‡]Department of Pharmacology, University of Pennsylvania Medical Center, Philadelphia, Pennsylvania 19104-6068, USA

ABSTRACT **Vascular immunotargeting, the administration of drugs conjugated with antibodies to endothelial surface antigens, has the potential for drug delivery to the endothelium. Our previous cell culture studies showed that biotinylated antibodies to PECAM-1 (a highly expressed endothelial surface antigen) coupled with streptavidin (SA, a cross-linking protein that facilitates anti-PECAM internalization and targeting) may provide a carrier for the intracellular delivery of therapeutic enzymes. This paper describes the PECAM-directed vascular immunotargeting of a reporter enzyme (β-galactosidase, β-Gal) in intact animals. Intravenous injection of [^{125}I]SA-β-Gal conjugated with either anti-PECAM or IgG led to a high ^{125}I uptake in liver and spleen, yet β-Gal activity in these organs rapidly declined to the background levels, suggesting rapid degradation of the conjugates. In contrast, anti-PECAM/[^{125}I]SA-β-Gal, but not IgG/[^{125}I]SA-β-Gal, accumulated in the lungs (36.0±1.3 vs. 3.9±0.6% injected dose/g) and induced a marked elevation of β-Gal activity in the lung tissue persisting for up to 8 h after injection (10-fold elevation 4 h postinjection). Using histochemical detection, the β-Gal activity in the lungs was detected in the endothelial cells of capillaries and large vessels. The anti-PECAM carrier also provided ^{125}I uptake and β-Gal activity in the renal glomeruli. Predominant intracellular localization of anti-PECAM/SA-β-Gal was documented in the PECAM-expressing cells in culture by confocal microscopy and in the pulmonary endothelium by electron microscopy. Therefore, vascular immunotargeting is a feasible strategy for cell-selective, intracellular delivery of an active foreign enzyme to endothelial cells *in vivo*, and thus may be potentially useful for the treatment of acute pulmonary or vascular diseases.—Scherpereel, A., Wiewrodt, R., Christofidou-Solomidou, M., Gervais, R., Murciano, J.-C., Albelda, S. M., Muzykantov, V. R. Cell-selective intracellular delivery of a foreign enzyme to endothelium *in vivo* using vascular immunotargeting. *FASEB J.* 15, 416–426 (2001)**

Key Words: drug targeting · lung · PECAM-1 · β-galactosidase · streptavidin

GENE THERAPY IS based on the premise that DNA can be delivered safely and efficiently to target cells within an organism to allow production of a desired protein. However, the direct intracellular delivery of foreign proteins would provide important and complementary opportunities for therapeutic and experimental interventions. For example, intracellular targeting of an active antioxidant enzyme could produce an effect more rapidly than transduction of the corresponding antioxidant gene, a feature required for the treatment of an acute pathological process such as ischemia/reperfusion injury.

Some progress has been made toward achieving effective routes for cellular entry of proteins (protein transduction). One approach uses genetically engineered fusion proteins using membrane-permeating peptides coupled to foreign enzymes (1–3). As an example, Schwarze et al. recently demonstrated the ubiquitous expression of an active enzyme *in vivo* after intraperitoneal injection of a denatured fusion protein composed of the protein transduction domain of the human immunodeficiency virus TAT protein fused to β-galactosidase (4). Although useful, this strategy currently lacks specificity, that is, protein expression cannot be targeted to a desired tissue. A potentially even more useful application of protein transduction would combine effective intracellular entry with cell-selective targeting of the desired protein *in vivo*.

Vascular immunotargeting theoretically offers such an approach (5, 6). The endothelium represents a large, accessible, and important therapeutic target for the treatment of a spectrum of cardiovascular and pulmonary diseases. However, a successful vascular immunotargeting strategy will depend on two processes. First, conjugates of effector compounds (e.g., enzymes) with antibodies against specific endothelial surface antigens must bind selectively to endothelium.

[1] The first two authors contributed equally to this paper.

[2] Correspondence: Institute of Environmental Medicine, University of Pennsylvania Medical Center, 1 John Morgan Building, 36th Street and Hamilton Walk, Philadelphia, PA 19104-6068, USA. E-mail: muzykant@mail.med.upenn.edu

0892-6638/01/0015-0416 © FASEB

Second, these conjugates must then become internalized and routed to an intracellular compartment that allows the active conjugated drug to act. Successful targeting of the conjugates to pulmonary endothelium has been demonstrated previously. Because of the extremely large surface area and effective circulation, carrier antibodies accumulate in the lungs and have been shown to bring about preferential pulmonary uptake of radiolabeled enzymes after intravenous (i.v.) administration in intact animals (6, 7, 8, 9). However, the second part of the process, intracellular delivery of an active enzyme, has not been demonstrated in intact animals.

Our recent studies show that antibodies to platelet endothelial cell adhesion molecule-1 (anti-PECAM) conjugated with streptavidin (SA, a biotin binding protein that cross-links biotinylated enzymes and antibodies) can serve as a carrier for intracellular delivery of conjugated foreign cargo compounds (such as enzymes and genes) to endothelium. We have found that streptavidin markedly facilitates intracellular uptake of anti-PECAM in endothelial cell culture *in vitro* and its pulmonary targeting *in vivo* in intact animals (9), and that glucose oxidase conjugated with anti-PECAM/SA carrier enters endothelial cells and generates H_2O_2 intracellularly in cell cultures (10). We have also observed that radiolabeled glucose oxidase conjugated with an anti-PECAM/SA carrier accumulate in the lungs after intravascular injection in intact animals (9, 11).

Based on these results, we postulated that anti-PECAM/SA could deliver active enzymes inside endothelial cells *in vivo*. In the present study we tested this hypothesis directly by characterizing the functional activity, along with the tissue and cellular localization using confocal and electron microscopy, of a reporter enzyme (β-galactosidase, β-Gal) conjugated to an anti-PECAM carrier. The results indicate that anti-PECAM permits cell-selective, intracellular delivery of an active foreign enzyme, β-Gal, to endothelium in cell culture and intact animals. The kinetics of this process were also defined. Our results validate the feasibility of vascular immunotargeting of enzymes and imply that this strategy may be useful for the treatment of acute pulmonary or vascular diseases.

MATERIALS AND METHODS

Antibodies and enzymes

Two antibody preparations were used: *1)* mAb 390, a rat mAb reacting with murine PECAM-1/CD31 (12); and *2)* nonspecific rat IgG (Calbiochem, San Diego, Calif.). The preparation of β-galactosidase covalently coupled to streptavidin (SA-β-Gal, with specific β-Gal activity 400 units/mg) was purchased from Sigma Chemicals (St. Louis, Mo.).

Biotinylation, radiolabeling, and conjugation of proteins

Proteins were biotinylated with 6-biotinylaminohexanoic acid *N*-hydroxysuccinimide ester (NHS-LC-Biotin, Pierce, Rockford, Ill.) without detectable reduction of their functional activity as described previously (6) and designated as b-IgG or b-anti-PECAM. Prior to conjugation with biotinylated proteins, SA-β-Gal was dissolved at 0.5 mg/ml in phosphate-buffered saline (PBS), pH 7.3 and labeled with ^{125}Iodine (NEN Dupont) using Iodogen (Pierce), according to a standard manufacturer's instructions. Either b-IgG or b-anti-PECAM was added dropwise to [^{125}I]SA-β-Gal in the vortex at room temperature (RT). The molar ratio [^{125}I]SA-β-Gal to biotinylated proteins varied from 0.25 to 2 in order to obtain nonaggregated, stable conjugates. Size of the resulting conjugates was determined using a Dynamic Light Scattering machine (Brookhaven Instruments, N.Y.), with 60°, 90°, and 120° angles. The radiolabeled conjugates are designated in the text as anti-PECAM/[^{125}I]SA-β-Gal or IgG/[^{125}I]SA-β-Gal, whereas nonlabeled counterparts are designated as anti-PECAM/SA-β-Gal and IgG/SA-β-Gal.

The measurement of β-Gal activity *in vitro* and *in vivo*

β-Galactosidase activity in the conjugate preparations, cell lysates, or organ homogenates was determined using a β-Gal enzyme assay kit from Promega (Madison, Wis.). Organs were homogenized in 3 ml of the reporter lysis buffer (RLB) 1× from the kit containing protease inhibitor mixture (10 μl/ml, Sigma) and centrifuged at 4°C, 4000 RPM (3000 *g*) for 45 min. Enzymatic β-Gal activity was determined in the supernatants at various dilutions. The BCA Protein Assay Kit (Pierce) was used to measure the protein concentration in the samples.

Binding and uptake of the conjugates in cell culture

Human mesothelioma REN cells transfected with cDNA encoding murine PECAM (REN/PECAM cells, obtained as described (13), were used in the study. Nontransfected REN cells served as a cell type-matched control. The conjugates were incubated with the cells in RPMI medium (GibcoBRL, Grand Island, N.Y.) with 10% fetal calf serum for 1 h at 37°C. Afterward, in some wells, according to the β-Gal enzyme assay protocol, cells were washed with PBS (Ca^{2+} and Mg^{2+} free) and incubated with RLB for 15 min at RT. The cell lysates were collected, centrifuged, and β-Gal activity was determined in the supernatants. In the parallel wells, cells were washed with RPMI and fixed with 2% paraformaldehyde for 10 min at RT. In some wells, cells were incubated for 10 min with 0.1% Triton X, in order to attain complete permeabilization of the plasma membrane. Permeabilized and nonpermeabilized cells were further incubated with rabbit antibody against β-Gal (1:250 dilution, 5Prime→ 3Prime, Inc., Boulder, Colo.), washed, and incubated with Texas red-labeled goat anti-rabbit antibody (1:250 dilution, Jackson ImmunoResearch Lab., Inc, Bar Harbor, Maine) for 30 min at RT, then washed with Dulbecco's PBS. Images were taken using a fluorescent microscope (Olympus, Tokyo, Japan) or using an inverted epifluorescence Nikon TE300 microscope with 60× oil-immersion objective, appropriate filter sets, and a confocal attachment (Radiance 2000, Bio-Rad, Hercules, Calif.).

Biodistribution and tissue localization of the conjugates in intact animals

The biodistribution of radiolabeled conjugates in animals was studied as described previously (6). One hour after the tail vein injection of anti-PECAM/[^{125}I]SA-β-Gal or IgG/[^{125}I]SA-β-Gal conjugates in anesthetized BALB/c mice (8 μg of [^{125}I]SA-β-Gal/animal), animals were killed, internal organs were harvested, rinsed with saline, and the ^{125}I in tissues

was determined in a gamma counter (Wallac-LKB). The lung is a very vascularized organ and as much as 10–15% of the wet lung weight may belong to a residual blood. Thus, theoretically, the value of lung-associated conjugate may be contaminated by the blood pool. However, in previous studies we observed that flushing of pulmonary vasculature with saline did not change significantly values of the specific pulmonary uptake of immunoconjugates in animals *in vivo* (6, 7). Thus, in the present study we did not flush lungs with saline. However, to account for potential contribution of the residual blood in every organ, we determined the blood level of ^{125}I in each experiment, calculated tissue-to-blood ratio (localization ratio), and compared this parameter for anti-PECAM/[^{125}I]SA-β-Gal or IgG/[^{125}I]SA-β-Gal conjugates.

The tissue localization of enzymatically active β-Gal in mice was studied by the β-Gal activity assay in the tissue homogenates and by histological analysis of X-Gal staining. After injection of 30–50 μg of the conjugates into the tail vein of BALB/c mice, animals were killed at different time intervals. The internal organs were cleared of blood by intra-cardiac injection of 20 ml of PBS via the right ventricle, harvested, and rinsed externally with PBS. Organs were frozen either in RLB for the β-Gal activity assay performed as described above or in OCT (VWR Scientific Products, Irving, Tex.) for the X-Gal staining. Frozen sections of tissues were rinsed in PBS, fixed in 0.5% glutaraldehyde, and incubated in X-Gal solution for 4 h at RT (14).

Electron microscopy of the endothelial uptake of anti-PECAM/SA-β-Gal conjugate

Routine embedding for immunoelectron microscopy

Lungs were fixed in ice-cold fixative (2% para-formaldehyde/0.1% glutaraldehyde) in 0.1 M cacodylate buffer pH 7.4 for 30 min, cut into 1 mm^3 pieces, and allowed to fix further under vacuum for several hours. After three washings in cacodylate buffer, lungs were incubated in 0.1 M glycine for 1 h at RT. Lungs were then washed three times with cacodylate buffer, followed by dehydration in a series of graded alcohols [15%, 35%, 70%, 95%, 100% (3×)] for 10 min in each step. Sections were infiltrated with LR White resin (EM Sciences, Malvern, Pa.) and allowed to polymerize at 55°C for 3 days.

Immunoelectron microscopy

Ultra-thin sections (100 nm) were cut with a diamond knife (Diatome, Switzerland) using a Leica ultra-microtome (Chicago, Ill.). LR White sections were collected on 200 mesh nickel grids (Electron Microscopy Sciences) and first rinsed on drops of water, followed by etching in 10% NaIO4 and 0.1 M HCl, each for 15 min, and then by blocking in 5% serum each for 15 min. Grids were floated on drops of PBS solution containing the primary antibody (rabbit polyclonal anti-β-Gal, 1:100 dilution) overnight at 4°C. Nonbound anti-β-Gal was washed with PBS containing 0.5% bovine serum albumin, 0.1% fish gelatin, and 0.05% Tween 20. Grids were floated for 30 min in the drops of PBS solution containing the secondary antibody (gold conjugated, goat-anti-rabbit IgG-Au$_{10}$, Amersham, 1:10 dilution). Sections were rinsed as described previously and postfixed in 2% glutaraldehyde/PBS for 2 min, followed by washing with water, and postcontrasted with 20% uranyl acetate/0.5% lead citrate. The sections were inspected in a Hitachi H-600 transmission electron microscope (Nissey Sangyo, Gaithersburg, Md.) at 75 KV.

Statistics

Analysis of statistically significant differences ($P<0.05$) between groups was performed using a *t* test or a one-way analysis of variance (SigmaStat 2.0.). *Post hoc* testing was performed using the Fischer least square difference test (7). If not otherwise indicated, all data are expressed as mean ± SE.

RESULTS

Synthesis of anti-PECAM/SA-β-Gal conjugates

Successful immunotargeting requires the production of stable, uniform, nonaggregated conjugates. To optimize size and stability of the conjugates, b-anti-PECAM or b-IgG were coupled to SA-β-Gal at molar ratios 0.25, 0.5, 0.75, 1, and 2. With the lowest molar ratio, immediate aggregation of the conjugates was observed (mean size > 2 μm). At higher molar ratios (including twofold molar excess of b-anti-PECAM), b-anti-PECAM and SA-β-Gal formed conjugates with diameter in the range of 60–180 nm. For the experiments described in this paper, we used the conjugate formed at b-anti-PECAM:SA-β-Gal molar ratio 0.75, designated below in the text as anti-PECAM/SA-β-Gal. The mean diameter of the b-anti-PECAM/SA-β-Gal was 121 ± 12 nm whereas that of the IgG/SA-β-Gal was 83 ± 8.1 nm (according to 90° DLS). Dynamic light scattering of the conjugates at various angles (60–90°) showed similar results, thus indicating that the conjugates are homogeneous in size. Determination of size in water and media with physiological salt concentrations gave similar results. The conjugates retained a stable size and full initial enzymatic activity of nonconjugated SA-β-Gal for at least 7 days at 4°C.

Binding of the conjugates to the target cells *in vitro*

To characterize the behavior of anti-PECAM/SA-β-Gal conjugates in an *in vitro* model of endothelium, we studied an endothelium-like cell line (human mesothelioma REN cells) transfected with murine PECAM. This model has advantages of stability, reproducibility, and allows the use of nontransfected REN cells as a cell type-matched negative control.

Figure 1 shows fluorescent microscope images of the conjugates binding to the cells revealed in the permeabilized cells after 1 h incubation by a polyclonal antibody directed against β-Gal (anti-β-Gal). The control conjugate, IgG/SA-β-Gal, showed no significant binding to either PECAM-negative or PECAM-positive cells (Fig. 1*A, B*). In contrast, intense cellular fluorescence was observed after binding of anti-PECAM/SA-β-Gal to REN/PECAM, but not control REN cells (compare panels *C* and *D*, Fig. 1). These data show the specificity of anti-PECAM/SA-β-Gal recognition of the antigen-positive cells.

To more precisely characterize the cellular localization of anti-PECAM/SA-β-Gal in REN/PECAM cells, we compared fluorescence images obtained with anti-β-Gal in nonpermeabilized vs. permeabilized cells (**Fig. 2**). Confocal microscope sections of the nonpermeabilized cells revealed bright fluores-

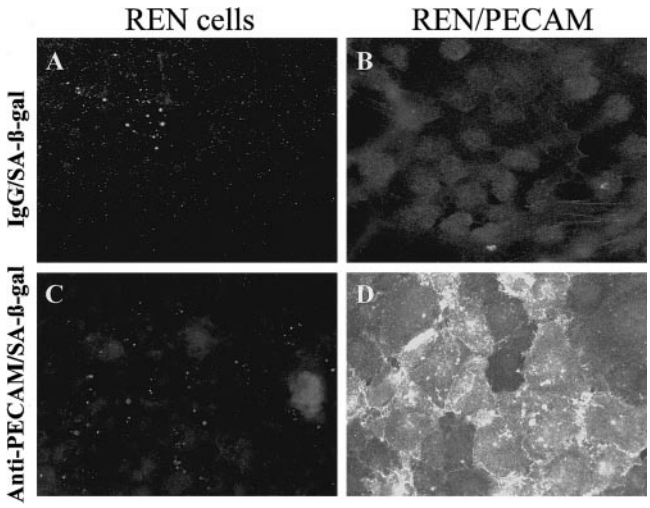

Figure 1. Selective binding of anti-PECAM/SA-β-Gal to PECAM-positive cells. IgG/SA-β-Gal (*A, B*) or anti-PECAM/SA-β-Gal (*C, D*) were incubated with REN cells (*A, C*) or REN cells transfected with PECAM-1 (*B, D*) for 1 h at 37°C. After elimination of nonbound conjugates, permeabilized fixed cells were sequentially incubated with a rabbit antibody against β-Gal and a Texas red-labeled goat anti-rabbit antibody. Images were taken in a fluorescent microscope (gain: 100; 20×).

cence on the luminal surface (Fig. 2*A*) and in the plasma membrane (Fig. 2*B*), but not in the intracellular compartment. In contrast, permeabilized cells displayed an intense intracellular anti-β-Gal fluorescence that increased with the depth of the cell sections (Fig. 2*C, D*). Therefore, REN/PECAM cells internalize anti-PECAM/SA-β-Gal.

Anti-PECAM/SA-β-Gal associated with REN/PECAM cells was enzymatically active (**Fig. 3**). After 1 h incubation of anti-PECAM/SA-β-Gal with REN/PECAM cells at 37°C, β-Gal activity in the wells attained 80 mU/mg, whereas it was an order of magnitude lower in the control wells (e.g., 8.6±0.2 mU/mg in REN cells). Likely due to the high sensitivity of the enzymatic assay, we detected a significant level of β-Gal activity in the REN/PECAM cells incubated with IgG/SA-β-Gal (~20 mU/mg). Nevertheless, it was fourfold lower than that in the REN/PECAM cells incubated with anti-PECAM/SA-β-Gal conjugate. Incubation of REN/PECAM cells (preincubated with anti-PECAM/SA-β-Gal for 1 h at 37°C) with a glycine buffer, pH 2.5 (an elution procedure that eliminates the surface-bound conjugate) led to only a 30% reduction of the cell-associated β-Gal activity (not shown). Together with the confocal microscopy pattern of anti-β-Gal staining shown on Fig. 2, these data indicate that *1)* REN/PECAM cells internalize the major proportion (~60–70%) of the cell-associated anti-PECAM/SA-β-Gal and *2)* intracellular β-Gal is active. These findings corroborate with our previous *in vitro* observations that endothelial and REN/PECAM cells internalize an active glucose oxidase conjugated with anti-PECAM/SA carrier (9, 10).

Immunotargeting of anti-PECAM/[^{125}I]SA-β-Gal to the vascular endothelium in intact animals

In the next series of experiments, we measured the uptake of [^{125}I]SA-β-Gal conjugated with either anti-PECAM or IgG in the internal organs of mice 1 h after i.v. administration (**Table 1**). The conjugates initially showed accumulation of ^{125}I in the liver [22–26% injected dose/g of tissue (% injected dose/g)] and spleen (13–15% injected dose/g). The hepatic and splenic immunospecificity index (ISI, ratio between the tissue uptake of immune and nonimmune counterparts) was close to 1. This result indicates equal uptake of the immune and nonimmune conjugates and likely reflects PECAM-independent, Fc receptor-mediated uptake by macrophages in these organs. Even though the blood level of the immune conjugate was similar to and did not exceed that of nonimmune counterpart, uptake of anti-PECAM/[^{125}I]SA-β-Gal doubled that of IgG/[^{125}I]SA-β-Gal in heart and kidney ($P<0.01$). Thus, renal and cardiac ISI attained a value of 2.3–2.5.

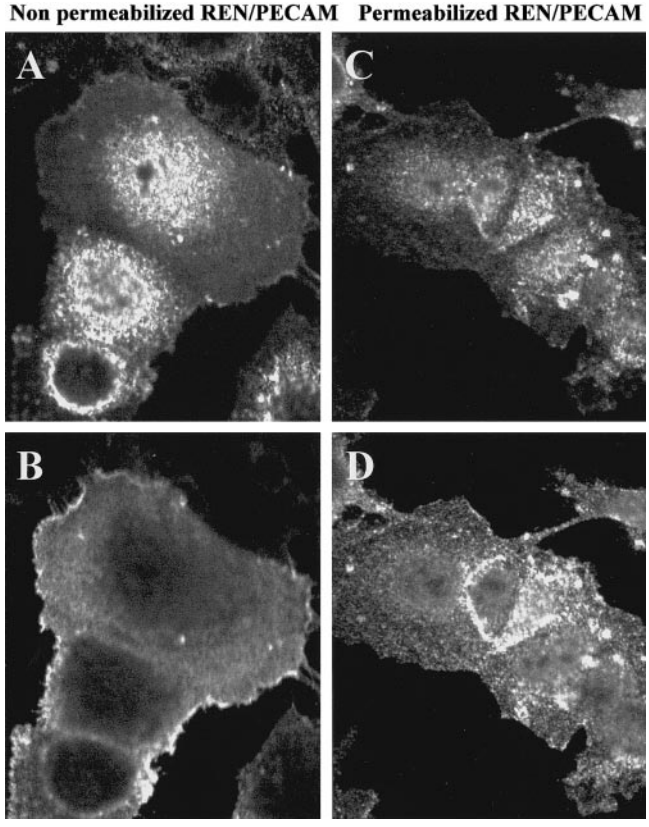

Figure 2. Internalization of anti-PECAM/SA-β-Gal by PECAM-positive cells. Anti-PECAM/SA-β-Gal was incubated with REN/PECAM cells for 1 h at 37°C. After elimination of nonbound conjugates, fixed (but nonpermeabilized) cells were sequentially incubated with a rabbit antibody against β-Gal and a Texas red-labeled goat anti-rabbit antibody. Images were obtained in a confocal microscope (20×). *A, B)* Cells not permeabilized prior to incubation with β-Gal antibody; *C, D*) cells that have been permeabilized. *A, C)* A confocal section close to the apical surface of the cell monolayer (~8 microns from the plastic well); *B, D)* section close to the cell median (~2.5 microns from the plastic well).

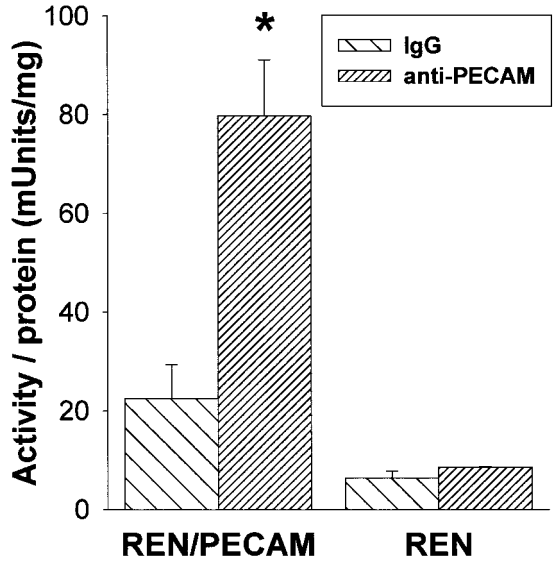

Figure 3. Targeting of enzymatically active anti-PECAM/SA-β-Gal to PECAM-positive cells. β-Gal activity assay in cells lysates expressed as mU/mg protein (M±SE; n=3). REN/PECAM cells incubated with anti-PECAM/SA-β-Gal (*) showed a significantly higher activity than the cells incubated with IgG/SA-β-Gal (P=0.01).

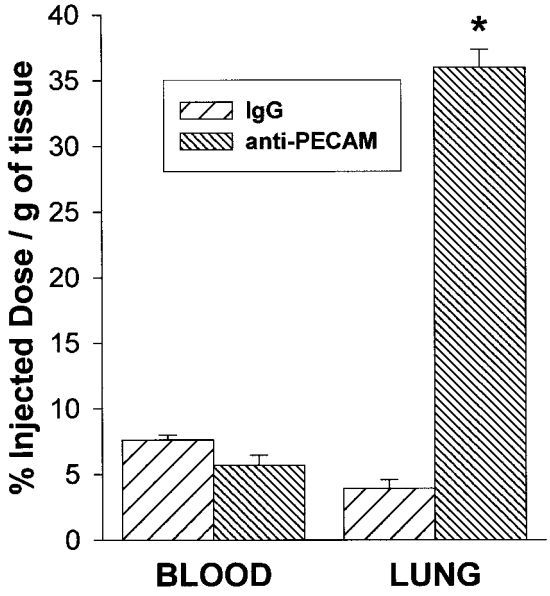

Figure 4. Pulmonary accumulation of anti-PECAM/[^{125}I]SA-β-Gal 1 h after tail vein injection in intact mice. The results are expressed as mean value ± SE (n=3); pulmonary uptake of anti-PECAM/[^{125}I]SA-β-Gal (*P<0.001) was significantly higher than that of IgG/[^{125}I]SA-β-Gal.

This result likely reflects binding of anti-PECAM/[^{125}I]SA-β-Gal to renal and cardiac endothelium. The most striking difference between the levels of tissue uptake of immune and nonimmune conjugates was observed in the lungs. The lung is the most vascularized organ in the body and endothelium-specific antibodies accumulate in the pulmonary vasculature (5–9). Level of ^{125}I in murine lungs was an order of magnitude higher after injection of anti-PECAM/[^{125}I]SA-β-Gal than IgG/[^{125}I]SA-β-Gal (**Fig. 4**). High pulmonary uptake of anti-PECAM/[^{125}I]SA-β-Gal cannot be explained by lung contamination with a residual blood, since blood levels of the anti-PECAM conjugate did not exceed that of the control IgG conjugate. To account for a residual blood, we calculated lung-to-blood ratio (localization ratio) for immune and nonimmune conjugates. The ratio of these two parameters gives the ISI (normalized to blood) that exceeds 10 (see Table 1). In fact, pulmonary uptake of the immune conjugate markedly exceeded that of any other organ, likely reflecting binding of the conjugate to the pulmonary endothelium. Thus, anti-PECAM/SA-β-Gal injected i.v. accumulates preferentially in the lungs.

Anti-PECAM/SA-β-Gal causes organ-selective elevation β-Gal activity *in vivo*

To evaluate whether anti-PECAM/SA carrier delivers enzyme to endothelium in an active form, β-Gal activity was measured in the internal organs after i.v. injection of the conjugates. **Table 2** shows the profile of β-Gal activity in various organs 1 and 4 h after conjugate injection. Similar to the ^{125}I distribution data, 1 h after injection of either the immune or nonimmune conjugate, significant β-Gal activity was detected in the liver

Table 1. *Biodistribution of anti-PECAM/[^{125}I]SA-β-Gal or IgG/[^{125}I]SA-β-Gal in intact mice 1 h after i.v. injection*[a]

Organ	%ID/g	%ID/g	ISI	Loc. ratio	Loc. ratio	ISI
	mAb/β-Gal	IgG/β-Gal		mAb/β-Gal	IgG/β-Gal	
Blood	5.7 ± 0.8	7.6 ± 0.4	0.74	1.0	1.0	1.0
Lung	**36.0 ± 1.3**	**3.9 ± 0.6**	**9.19**	**6.5 ± 0.6**	**0.5 ± 0.1**	**12.7**
Heart	5.0 ± 1.0	2.6 ± 0.3	1.90	0.9 ± 0.1	0.3 ± 0.1	2.5
Liver	21.8 ± 3.3	26.5 ± 1.5	0.82	3.8 ± 0.1	3.5 ± 0.2	1.1
Spleen	15.4 ± 1.8	12.5 ± 1.3	1.23	2.8 ± 0.5	1.66 ± 0.3	1.7
Kidney	7.1 ± 0.7	4.2 ± 0.2	1.68	1.3 ± 0.1	0.5 ± 0.1	2.3

[a] Intact mice were injected via tail vein with 8 μg of [^{125}I]SA-β-Gal conjugated with either anti-PECAM (n=3) or rat IgG (n=3). The table shows biodistribution of [^{125}I] in organs 1 h after injection, M ± SE. The data are shown as a percent of injected dose per gram of tissue (% ID/g) and as localization ratio (Loc. Ratio), which is ratio of the radioactivity per gram of a tissue to that of blood. The immunospecificity index (ISI) is calculated as ratio between anti-PECAM/[^{125}I]SA-β-Gal and IgG/[^{125}I]SA-β-Gal using either % ID/g or Loc. Ratio. The latter method of ISI calculation compensates for a difference in blood level of the immune and nonimmune conjugates. Both methods of calculating ISI give similar results.

Table 2. *Increase of β-galactosidase activity measured in vivo*[a]

Time after injection	1 h		4 h	
	anti-PECAM	IgG	anti-PECAM	IgG
Lung	**17.2 ± 1.8***	2.2 ± 0.7	**10.6 ± 1.2****	2.1 ± 1.2
Liver	14.4 ± 1.3	16.8 ± 1.7	1.4 ± 0.2	—
Spleen	7.7 ± 0.5	3.8 ± 0.4	1.9 ± 0.2	1.7 ± 0.3
Kidney	5.5 ± 0.8	2.4 ± 0.9	1.9 ± 0.1	0.7 ± 0.1

[a] SA-β-Gal (40 μg) conjugated either to anti-PECAM mAb (n=8) or IgG (n=4) was injected into the vein tail in BALB/c mice. A control group included intact mice. Organs were washed to remove blood, flash frozen, and then homogenized. Results are shown as the ratio of the value of the β-Gal activity in the tissue homogenate (in mUnits of β-Gal activity/mg of protein) to the value of the control group (2.1±0.3 mU/mg in the lungs) (M±SE, N=8). Both at 1 hr and 4 hrs post injection, activity measured in the lungs was significantly higher after injection of anti-PECAM/SA-β-Gal than in the IgG/SA-β-Gal group (* P<0.001; ** P=0.003).

and spleen. The renal β-Gal activity after anti-PECAM/SA-β-Gal injection doubled that seen after IgG/SA-β-Gal injection. Again, the most striking difference between the immune and nonimmune conjugates was observed in the lung. After anti-PECAM/SA-β-Gal injection, pulmonary β-Gal activity attained the highest level of any organ and exceeded that seen after IgG/SA-β-Gal injection by an order of magnitude. No significant β-Gal activity was observed in the lungs after injection of nonconjugated SA-β-Gal (data not shown).

β-Gal activity in the liver and spleen was reduced to a background level during the time interval from 1 to 4 h postinjection. One explanation for this rapid decline of activity is that the conjugates are degraded by the resident reticuloendothelial system cells. In contrast, β-Gal activity in the lung tissue was reduced by only 30% during this time interval and still was an order of magnitude higher than the control level (Table 2). The specific (i.e., provided by anti-PECAM/SA-β-Gal, but not IgG/SA-β-Gal) and prolonged character of β-Gal activity in the lung, together with its localization in the tissue (see below), implies that anti-PECAM delivers active β-Gal to the pulmonary vascular endothelium.

Figure 5 compares the kinetics of β-Gal activity in the lung and spleen. Anti-PECAM/SA-β-Gal i.v. injection caused very rapid elevation of β-Gal activity in both organs, reaching a peak level 15–20 min postinjection. However, in contrast to a rapid decline of β-Gal activity in spleen, pulmonary β-Gal activity displayed a two-phase decline: a rapid reduction to 50% of the peak level within first hour, followed by a slower reduction (to 30% of the peak level 4 h postinjection). As long as 8 h postinjection, β-Gal activity in the lung tissue remained at an elevated level (almost threefold higher than the background level, P<0.01). One day after a single bolus injection of anti-PECAM/SA-β-Gal conjugate, β-Gal activity in the lung tissue returned to a background level.

These data indicate that i.v. administration of anti-PECAM/β-Gal causes a more prominent and more persistent elevation of β-Gal activity in the lungs than in other organs. Enzymatic activity in the lung was detectable for at least 8 h after injection.

Endothelial localization of β-Gal activity *in vivo*

To define the tissue localization of active β-Gal in the lung and other organs, frozen sections of the organs were analyzed after standard X-gal staining. **Figure 6** shows representative results of this analysis in organs harvested 4 h after conjugate injection. Consistent with the quantitative data shown in Table 2, minimal β-Gal activity was detected in the sections of the liver tissue 4 h postinjection of either anti-PECAM/SA-β-Gal or IgG/SA-β-Gal. Residual β-Gal activity was detected at the periphery of the follicles in specific areas of the spleen. This activity was presumably due to nonspecific uptake, since the pattern of staining was similar for anti-PECAM/SA-β-Gal and IgG/SA-β-Gal. In the kidney tissue sections, specific β-Gal activity was detected in the renal glomeruli and in the lumen of blood vessels after injection of anti-PECAM/SA-β-Gal, but not IgG/SA-β-Gal. Intense β-Gal activity was detected in the lung tissue after injection of anti-PECAM/SA-β-Gal, but not IgG/SA-β-Gal.

The photomicrographs shown in **Fig. 7** illustrate points relating to the localization of β-Gal activity in the

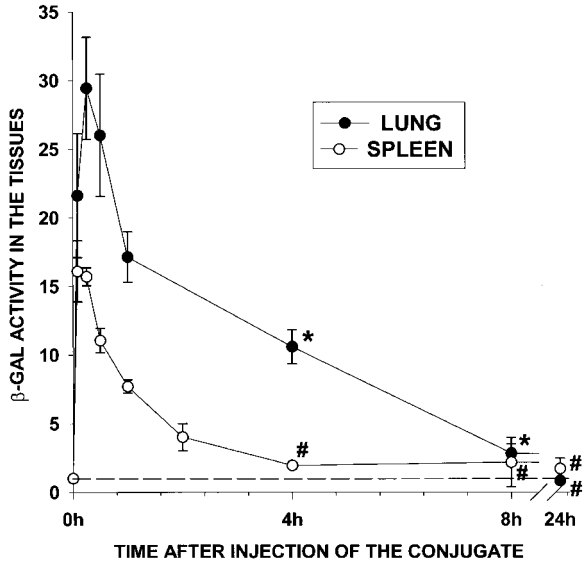

Figure 5. Kinetics of β-Gal enzymatic activity in the lung and spleen after i.v. injection of anti-PECAM/SA-β-Gal. Enzymatic β-Gal activity determined in the homogenates of either the lungs or the spleen harvested from mice injected with 50 μg of the conjugate is expressed as ratio to the background level of β-Gal activity in the same organ homogenates from intact mice (2.1 ± 0.3 β-Gal mU/mg of protein in the lung). The results are presented as mean ± SE (n=4–8). Within the first hour after injection, the values of β-Gal activity both in lung and spleen were statistically significantly higher than the background level (dash line). Note that β-Gal activity in the lungs was significantly higher than background value 8 h postinjection of the conjugate (*P<0.01). There was no significant β-Gal activity in the spleen 4 h and in the lung 24 h postinjection (#).

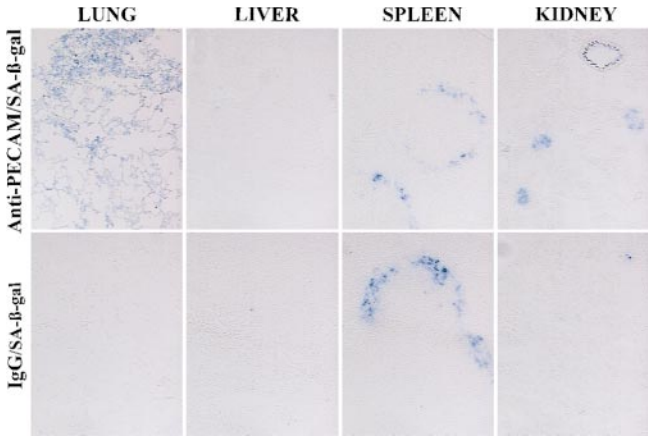

Figure 6. Tissue localization of β-Gal activity after injection of anti-PECAM/SA-β-Gal. Conjugates of anti-PECAM/SA-β-Gal or IgG/SA-β-Gal (50 μg SA-β-Gal/mouse) were injected into tail veins. Organs were harvested 4 h after injection and reacted with X-Gal to visualize enzymatic activity. 20×. Note extensive homogeneous X-Gal staining in the lung tissue and specific X-Gal staining in the renal blood vessels and glomeruli after injection of anti-PECAM/SA-β-Gal.

lungs after injection of anti-PECAM/SA-β-Gal. First, β-Gal activity was homogeneously disseminated throughout the highly vascularized alveolar compartment containing the major fraction of the pulmonary capillaries (Fig. 7*A*). Second, β-Gal activity was also detected in the lumen, but not in the tunica media and adventitia of large blood vessels (Fig. 7*A, C*). Third, no β-Gal activity was detected in the airways and interstitial compartments (Fig. 7*B*). Therefore, these data indicate that anti-PECAM carrier delivers an active β-Gal selectively to endothelium in intact animals. Endothelial cells in pulmonary vasculature and the glomerular capillaries seem to be preferential targets for the PECAM-directed delivery after i.v. administration.

Intracellular uptake of anti-PECAM/SA-β-Gal in pulmonary endothelium *in vivo*

To determine the subcellular localization of β-Gal in the lungs, we used immuno-gold electron microscopy with a β-Gal antibody. Rare cases of binding of gold particles to white blood cells in the pulmonary vessels were observed after injection of the conjugates, likely reflecting Fc receptor-mediated uptake by resident leukocytes (see as an example in **Fig. 8*A***). No specific binding of gold particles in the lung tissue could be detected after injection of saline or IgG/SA-β-Gal (data not shown). Rare gold particles found in the lung tissue (no more than one or two particles per field) could not be attributed to any specific structure in the lung tissue. This result corroborates with the data documenting low levels of the pulmonary uptake of IgG/SA-β-Gal (see Tables 1 and 2) and confirms the specificity of secondary anti-β-Gal and immuno-gold conjugate used in the study.

Figure 8 shows the typical patterns of the immuno-gold particles binding to sections of murine lungs obtained after anti-PECAM/β-Gal injection. In this type of experiment (as opposed to direct staining of tissue sections with primary and secondary antibodies), only a portion of antigen molecules can accommodate the conjugate and gold particles. Therefore, one could expect a relatively modest labeling of the tissue. However, as many as 20–30 gold particles could be detected per capillary vessel in most of the fields, revealing anti-PECAM/β-Gal in the pulmonary vasculature. Only rare gold particles were found in association with epithelial cells, red blood cells or components of the interstitial compartment. This result confirms that anti-PECAM carrier delivers β-Gal selectively to the endothelial cells. In contrast, numerous gold particles could be found in association with endothelial cells. We were able to visualize three patterns of immuno-gold labeling of endothelial cells. First, some gold particles were associated with endothelial plasma membrane (labeled as small arrowheads in Fig. 8*A–D*). Even in relatively clear areas (see Fig. 8*D*), the resolution of our method did not allow us to attribute these single particles to either intracellular or extracellular compartment. Second, small clusters of gold particles were localized in the endothelial junctions (indicated as large arrows), the site of preferential PECAM expression in the endothelial cells and likely site of the cellular entry for the anti-PECAM/SA-β-Gal conjugate (see Fig. 8*B*). Finally, the most common pattern was the presence of numerous gold particles and their clusters localized in the intracellular endothelial vacuoles, indicated by large arrowheads (Fig. 8*A–C*). For example, Fig. 8*A* outlines a cross section of a pulmonary capillary vessel. The insert clearly shows a large vesicular structure in the endothelial cell filled with gold particles. In fact, 38 of a total of 43 gold particles associated with this cell localize in this vesicle. This type of vesicular structure filled with conjugate was a common finding in the lung sections. Particles associated with the plasma membrane invaginations and vacuoles in the cytoplasm imply that the endothelial cells are actively internalizing the conjugate. In general, electron microscopy findings in the lung tissue after injection of anti-PECAM/SA-β-Gal were similar to those in the endothelial cells incubated with anti-PECAM/SA/ferritin in cell culture (9); both revealed internalization of anti-PECAM conjugates by endothelial cells. Therefore, the results of electron microscopy indicate that *1)* anti-PECAM delivers β-Gal selectively to the endothelial cells and *2)* a significant proportion of the delivered enzyme undergoes intracellular uptake.

DISCUSSION

Vascular immunotargeting, the administration of drugs, enzymes, or genetic material conjugated with antibodies directed against endothelial surface antigens (such as angiotensin-converting enzyme, thrombomodulin, PECAM, ICAM-1 or E-selectin), has the potential for cell-selective drug delivery to the endothe-

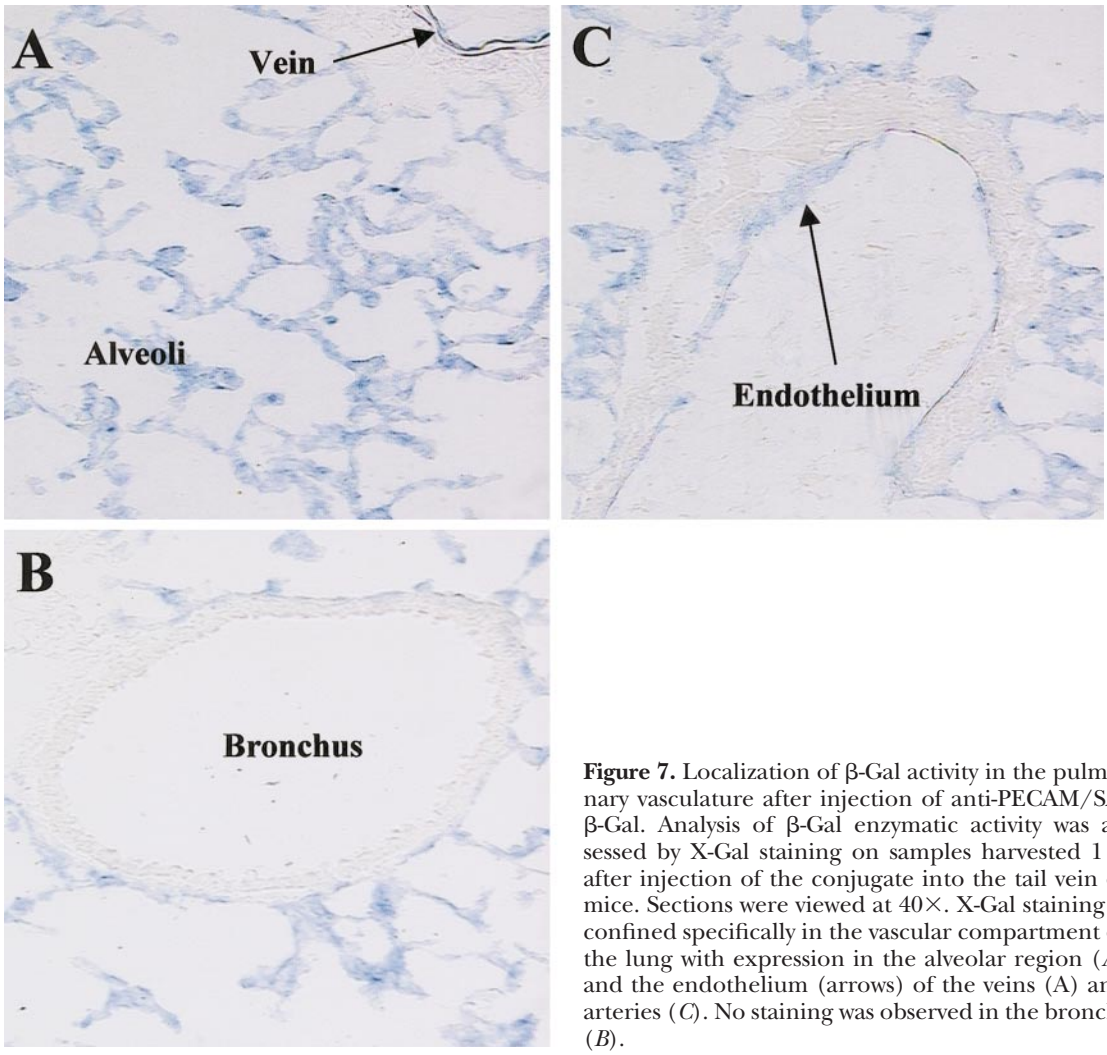

Figure 7. Localization of β-Gal activity in the pulmonary vasculature after injection of anti-PECAM/SA-β-Gal. Analysis of β-Gal enzymatic activity was assessed by X-Gal staining on samples harvested 1 h after injection of the conjugate into the tail vein of mice. Sections were viewed at 40×. X-Gal staining is confined specifically in the vascular compartment of the lung with expression in the alveolar region (*A*) and the endothelium (arrows) of the veins (A) and arteries (*C*). No staining was observed in the bronchi (*B*).

lium (6, 7, 8, 9, 15, 16). We and others have shown that selective pulmonary delivery of radiolabeled conjugates is possible (6–9). Very recently, we have also generated data in mice using anti-PECAM/SA conjugates of glucose oxidase (GOX, a H_2O_2-producing enzyme) to show that functional enzymes can be delivered to the lung using this approach. We found that anti-PECAM/SA/GOX accumulated in the lungs after i.v. injection and caused severe oxidative injury in the pulmonary vasculature (11). However, rapid and extensive injury caused by H_2O_2 generated in the lung made the visualization of the enzyme and kinetic studies of activity of the targeted enzyme impossible. Thus, to date, a number of questions that are key to the ultimate utility of vascular immunotargeting remain unanswered. These include *1)* the precise tissue localization of the delivered conjugates, *2)* the ability of the conjugates to move intracellularly *in vivo*, and *3)* the time course and kinetics of enzymatic activity after conjugate delivery.

To answer these questions, we studied the delivery of a well-characterized reporter enzyme, β-galactosidase, which allows measurement of its activity and localization in tissues. Using this approach, we could show that *1)* anti-PECAM/SA-β-Gal recognizes the vascular endothelium and accumulates preferentially in the lungs after i.v. administration; *2*) endothelium-associated β-Gal displays high enzymatic activity that is detectable within several minutes after a single bolus injection and lasts for at least 8 h, and *3)* a proportion of the injected β-Gal conjugates appear to accumulate inside the endothelial cells in cell culture and likely *in vivo*. This study, therefore, demonstrates for the first time that vascular immunotargeting can permit cell-selective, intracellular delivery of an active foreign enzyme to endothelium in intact animals.

The ability to actually visualize and track the localization of active enzyme provides some important insights. Clearly, the endothelium of the lung represents a major target for the conjugates. The distribution of enzyme was homogeneous: both large and small vessel endothelium showed activity. The other area to show specific uptake was the glomerular region of the kidney. A rapid, nonspecific uptake of both anti-PECAM and control IgG conjugates was seen in liver and spleen. This result is not surprising, given the major role of these organs in the clearance of immune complexes. In fact, all radiolabeled antibody- or IgG-based conjugates tested in our and other laboratories have displayed high hepatic and splenic uptake (6–9). However, β-Gal

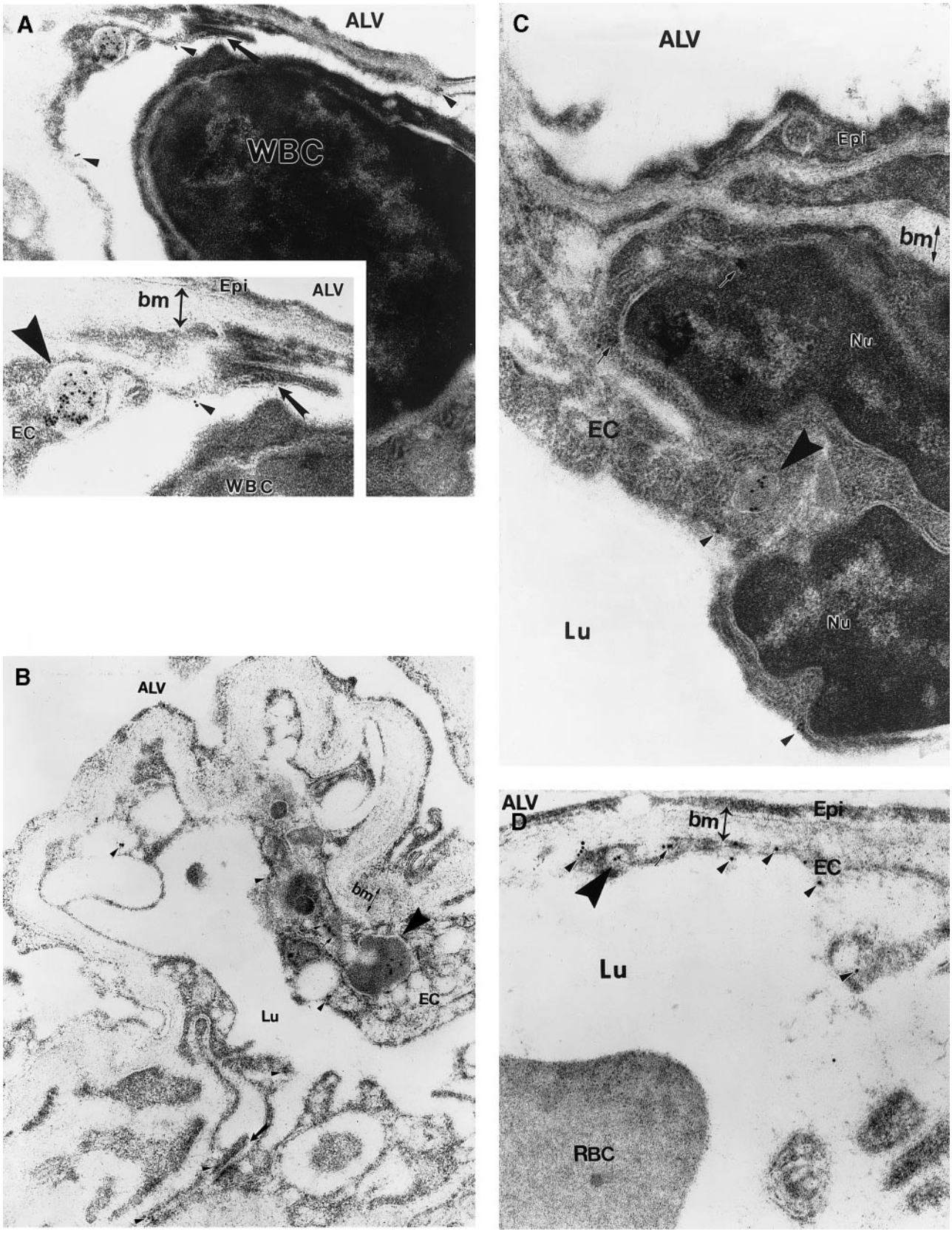

Figure 8. Intracellular delivery of β-Gal by anti-PECAM/SA-β-Gal in the pulmonary endothelium. Tissue sections of mouse lungs, harvested 1 h after i.v. injection of anti-PECAM/SA-β-Gal conjugate, were treated with antibody against β-Gal and secondary gold-conjugated antibody as described in Materials and Methods. Labels: RBC: red blood cell; WBC: white blood cell, EC: endothelial cell; bm: endothelial basal membrane; Lu: vascular lumen; ALV: alveolar space; Epi: alveolar epithelium; large arrows: endothelial cell junctions; small arrows: intracellular gold particles; small arrowheads: gold particles associated with endothelial cells; large arrowheads: endothelial vesicles.

enzymatic activity in these organs was very short-lived compared to the lung. We postulate that this is due to rapid Fc receptor-mediated uptake and degradation of the conjugates by the 'professional' phagocytes residing in the liver and spleen. Additional evidence to indicate that the fate of the internalized conjugates is different in liver and spleen vs. lung and kidney is provided by our recent study using anti-PECAM/GOX conjugates (11). In this study, marked hepatic and splenic uptake of both anti-PECAM/[^{125}I]GOX and IgG/[^{125}I]GOX was noted 1 h postinjection, yet these organs remained uninjured. The injury was induced only by antiPECAM/GOX and was localized in the lung (the organ where anti-PECAM/[^{125}I]GOX, but not IgG/[^{125}I]GOX, displayed a preferential uptake) and, to a lesser extent, in the renal glomeruli (11).

A prolonged, two-phase decrease of the conjugate activity in the lung may be explained in several ways. It could perhaps reflect a 'reutilization' or reuptake of the conjugate released by liver and spleen. We do not favor this scenario because the conjugate would likely loose its antigen binding and enzymatic activity after passage through macrophages in these organs. Another possibility is that an initial rapid phase of pulmonary degradation is due to uptake and degradation of the conjugate by resident mononuclear cells or macrophages in the lungs (see, for example, Fig. 8*A*). However, the very homogeneous distribution of the conjugate throughout the pulmonary vasculature (Fig. 7*A*) indirectly argues against this scenario. Another explanation could be a two-component mechanism of the conjugate degradation in the pulmonary endothelium (e.g., one rapid, such as the lysosomal pathway, and another that is slower). The mechanism(s) of the conjugate degradation in the lung is not clear at the present time, but it may be different for different types of conjugated enzymes. The topic represents a subject for more in-depth investigation. Nevertheless, our results clearly indicate that the anti-PECAM-conjugated reporter enzyme displays significant activity in the pulmonary vasculature for at least many hours after i.v. administration. This time interval may be sufficient to complement a gene delivery system.

The generalizability of these observations is an area of active investigation. In the present study, we used antibodies directed against PECAM-1 to provide immunotargeting to lung endothelial cells. PECAM-1 was chosen because *1)* it is highly expressed on the surface of endothelium; *2)* it mediates transmigration of leukocytes from blood to the tissues; and *3)* inflammatory mediators do not suppress its expression by endothelium (17). Blocking of PECAM by antibodies or conjugates may inhibit leukocyte infiltration and provide a secondary therapeutic benefit in inflammatory settings (18). Preliminary studies also indicate that, at least in part, pulmonary deposition of anti-PECAM conjugate is a 'first-pass' phenomenon and that selective catheterization may facilitate vascular delivery to specific organs such as the heart. However, other targeting antibodies have also been evaluated and appear to function as effective carriers (5). For example, we and others have successfully used anti-ACE and anti-thrombomodulin antibodies to deliver radiolabeled enzymes to pulmonary endothelium in rat and mouse models, although the tissue localization and functional activity of the delivered enzymes remain to be characterized (5, 7, 8).

The choice of targeted enzymes and the physical structure of the conjugates also require further study. Our preliminary data from *in vitro* studies suggest that the majority of conjugated enzyme is initially trafficked to large vacuoles that eventually fuse with lysosomes. Enzymes that generate or detoxify highly diffusible oxidants (such as hydrogen peroxide) may be well suited for this type of delivery, as precise cytoplasmic localization may not be necessary. There are, however, data that conjugates can escape from lysosomes and move to other cellular compartments, such as the nucleus. We have generated anti-PECAM/polylysine/green fluorescent protein DNA conjugates that selectively transfect PECAM-1-expressing cells (19). Effective delivery of conjugates may also depend on the size and aggregation status of the conjugates. Analysis of conjugate size using dynamic light scattering has indicated that smaller particles (~100–200 nm in diameter) are more efficient in intracellular delivery of enzymes *in vitro*. Studies to correlate size and delivery destination/efficiency *in vivo* are under way.

The ability to transiently deliver active enzymes at high levels to the vasculature has a number of potentially important therapeutic implications. For example, conjugates of antioxidant enzymes such as catalase or superoxide dismutase could be perfused prophylactically through donor organs to modulate ischemia/reperfusion injury associated with transplantation. Endothelial oxidant injury is also thought to play a major role in a number of other pulmonary diseases such as acute respiratory distress syndrome, radiation lung injury and oxygen toxicity and could thus potentially be approached using this technology.

In conclusion, our data indicate that anti-PECAM carrier permits cell-selective, intracellular delivery of an active foreign enzyme to endothelium in intact animals. These results validate the feasibility of vascular immunotargeting of enzymes and suggests that this strategy

A) 31,000×. An overview of the cross section of the pulmonary small blood vessel with WBC in the lumen and an adjacent alveolar space. Insert (58,000×) shows a large number of gold particles localized inside the endothelial cell. *B)* 60,000×. A cross section of the blood vessel in the lung shows a detailed view of the EC that selectively internalized the conjugate. Note the gold particles associated with a large endothelial vesicle. A small cluster of gold particles is also seen at the cell–cell junction (arrows). *C)* 60,000×. Note gold particles associated with an endothelial vesicle (big arrowhead), close to the cell nucleus. *D)* 68,000×. A detailed view of the endothelial cell separating vascular and alveolar space. Note numerous gold particles associated with EC, but not other cells and lung tissue structures.

may be useful for the treatment of acute pulmonary or vascular diseases. FJ

A.S. is a research fellow of the INSERM Unit U416 of the Pasteur Institute (Lille, France) supported by Pulmonary Society of French Language and Philippe Foundation Grants and the Hospital of Lille II University. R.W is a postdoctoral fellow of the Mildred Scheel Stiftung fuer Krebsforschung der Deutschen Krebshilfe e.V. (grant D/98/02288). This study was supported by the American Heart Association Established Investigator Grant (grant 9640204 to V.R.M.) and SCOR in Acute Lung Injury from National Institutes of Health Heart, Lung, and Blood Institute (HL 60290 Project 4 to V.R.M. and S.M.A.). We thank Evguenia Arguiris, Anu Thomas, Mildred Daise, and Kathleen Notarfrancesco for their invaluable technical expertise.

REFERENCES

1. Fawell, S., Seery, J., Dajkh, Y., Moore, C., Chen, L. L., Pepinsky, B., and Barsoum, B. (1994) Tat-mediated delivery of heterologous proteins into cells. *Proc. Natl. Acad. Sci. USA* **91,** 664–668
2. Liu, X. Y., Timmons, S., Lin, Y.-Z., and Hawinger, J. (1996) Identification of a functionally important sequence in the cytoplasmic tail of integrin β_3 by using cell-permeable peptide analogs. *Proc. Natl. Acad. Sci. USA* **93,** 11819–11824
3. Nagahara, H., Vocero-Akbani, A., Snyder, E., Ho, A., Latham, D., Lissy, N., Becker-Hapak, M., Ezhevsky, S., and Dowdy, S. (1998) Transduction of full-length TAT fusion proteins into mammalian cells: TAT-p27Kip1 induces cell migration. *Nature Med.* **4,** 1449–1452
4. Schwarze, S. R., Ho, A., Vocero-Akbani, A., and Dowdy, S. F. (1999) In vivo protein transduction delivery of a biologically active protein into the mouse. *Science* **285,** 1569–1572
5. Muzykantov, V. (1998) Immunotargeting of drugs to the pulmonary vascular endothelium as a therapeutic strategy. *Pathophysiology* **5,** 15–33
6. Muzykantov, V., Atochina, E., Ischiropoulos, H., Danilov, S., and Fisher, A. (1996) Immunotargeting of antioxidant enzymes to the pulmonary endothelium. *Proc. Natl. Acad. Sci. USA* **93,** 5213–5218
7. Danilov, S., Muzykantov, V., Martynov, A., Atochina, E., Sakharov, I., Trakht, I., and Smirnov, V. (1991) Lung is the target organ for a monoclonal antibody to ACE. *Lab. Invest.* **64,** 118–124
8. Maruyama, K., Kennel, S., and Huang, L. (1990) Lipid composition is important for highly efficient target binding and retention of immunoliposomes. *Proc. Natl. Acad. Sci. USA* **87,** 5744–5748
9. Muzykantov, V., Christofidou-Solomidou, M., Balyasnikova, I., Harshaw, D., Schultz, L., Fisher, A., and Albelda, S. (1999) Streptavidin facilitates internalization and pulmonary targeting of an anti-endothelial cell antibody (PECAM-1): a strategy for vascular immunotargeting of drugs. *Proc. Natl. Acad. Sci. USA* **96,** 2379–2384
10. Gow, A., Branco, F., Christofidou-Solomidou, M., Black-Schultz, L., Albelda, S., and Muzykantov, V. (2000) Immunotargeting of glucose oxidase: intracellular production of H_2O_2 and endothelial oxidative stress. *Am. J. Physiol.* **277,** L271–L281
11. Christofidou-Solomidou, M., Pietra, G., Solomides, C. S., Arguiris, E., Harshaw, D., Fitzgerald, G., Albelda, S., and Muzykantov, V. (1999) Immunotargeting of glucose oxidase to endothelium in vivo causes oxidative vascular injury in the lungs. *Am. J. Physiol.* **278,** L794–L805
12. Yan, H.-C., Pilewski, J., Zhang, Q., DeLisser, H., Romer, L., and Albelda, S. (1995) Localization of multiple functional domains on human PECAM-1 (CD31) by monoclonal antibody epitope mapping. *Cell Adhes. Comm.* **3,** 45–66
13. Gurubhagavatula, I., Amrani, Y., Pratico, D., Ruberg, F., Albelda, S., and Panittieri, R. (1998) Engagement of human PECAM-1 (CD31) on human endothelial cells increases intracellular calcium ion concentration and stimulates prostacyclin release. *J. Clin. Invest.* **101,** 212–222
14. Kucharczuck, J., Elshami, A., Zhang, H., Roy Smythe, W., Hwang, H., Tomlinson, J., Amin, K., Litzky, L., Albelda, S., and Kaiser, L. (1995) Pleural-based mesothelioma in immune competent rats: a model to study adenoviral gene transfer. *Ann. Thorac. Surg.* **60,** 593–598
15. Spragg, D., Alford, D., Greferath, R., Larsen, C., Lee, K., Gurthner, G., Cybulsky, M., Tosi, F., Nicolau, C., and Gimbrone, M. (1997) Immunotargeting of liposomes to activated vascular endothelial cells: a strategy for site-selective delivery in the cardio-vascular system. *Proc. Natl. Acad. Sci. USA* **94,** 8795–8800
16. Atochina, E., Balyasnikova, I., Danilov, S., Granger, D., Fisher, A., and Muzykantov, V. (1998) Immunotargeting of catalase to ACE or ICAM-1 protects perfused rat lungs against oxidative stress. *Am. J. Physiol.* **19,** L806–L817
17. Newman, P. (1997) The biology of PECAM-1. *J. Clin. Invest.* **99,** 3–8
18. Vaporician, A., Delisser, H., Yan, H., Mendiguren, I., Thom, S., Jones, M., Ward, P., and Albelda, S. (1993) Involvement of PECAM-1 in neutrophil recruitment in vivo. *Science* **262,** 1580–1582
19. Wiewrodt, R., Campbell, C. D., Feinstein, S. I., Schaffer, D., Albelda, S., and Muzykantov, V. (1999) PECAM-directed intracellular immunotargeting of genes. *Am. J. Resp. Crit. Care Med.* **159,** A347

Received for publication January 21, 2000.
Revised for publication August 2, 2000.